

Journal of
**Micro/Nanolithography,
MEMS, and MOEMS**

Nanolithography.SPIEDigitalLibrary.org

Fabrication of high-aspect ratio silicon nanopillars for tribological experiments

Pavlo V. Antonov
Marc R. Zuiddam
Joost W.M. Frenken

Fabrication of high-aspect ratio silicon nanopillars for tribological experiments

Pavlo V. Antonov,^{a,b,*†} Marc R. Zuiddam,^c and Joost W.M. Frenken^{a,b}

^aLeiden University, Huygens-Kamerlingh Onnes Laboratory, Niels Bohrweg 2, Leiden, 2233 CA, The Netherlands

^bAdvanced Research Center for Nanolithography, Science Park 110, Amsterdam, 1098 XG, The Netherlands

^cDelft University of Technology, Kavli NanoLab, Lorentzweg 1, Delft, 2628 CJ, The Netherlands

Abstract. This article reports the results of the fabrication of large arrays of nanopillars for future tribological experiments. This fabrication focused on achieving a constant high aspect ratio up to 1:24 and a separation between each pair of adjacent pillars. Electron beam lithography was used to write patterns in hydrogen silsesquioxane (HSQ) negative tone resist. To achieve nanopillars of high aspect ratios and with smooth sides, deep reactive ion etching was employed with SF₆ and O₂ at cryogenic temperatures. Finally, the residual HSQ was removed using CHF₃/O₂ plasma etching in order to obtain a smooth finish. © The Authors. Published by SPIE under a Creative Commons Attribution 3.0 Unported License. Distribution or reproduction of this work in whole or in part requires full attribution of the original publication, including its DOI. [DOI: [10.1117/1.JMM.14.4.044506](https://doi.org/10.1117/1.JMM.14.4.044506)]

Keywords: nanolithography; nanopillars; silicon; plasma etching; tribology.

Paper 15119 received Jul. 23, 2015; accepted for publication Nov. 10, 2015; published online Dec. 10, 2015.

1 Introduction

Over the past decade, nanostructured surfaces have become widely used in electronics,¹ biomedicine,² photonic crystals,³ battery technology,⁴ solar cells,⁵ etc. Independently of the area of application, the most important points of interest of nanofabrication control are the shapes that can be manufactured, including the aspect ratio of extreme shapes such as nanopillars, and the reproducibility with which the final structures can be produced. We report the fabrication of well-ordered nanopillar arrays for tribological applications. We utilize their mechanical properties in an attempt to influence the friction between dry and unlubricated surfaces. We expect friction to be affected significantly by the simultaneous and spontaneous motion of the nanopillars. We choose the dimensions of the nanopillars such that they exhibit transverse vibrations with an extremely high natural frequency of several GHz and above, in combination with a significant vibration amplitude at room temperature, typically on the order of an interatomic distance. Under these conditions, we foresee that when the nanopillars are brought into mechanical contact with a flat counter-surface, each nanopillar will conduct an independent, diffusive random walk over the counter-surface. This should reduce the lateral force required to translate the nanopillar array over the counter-surface to nearly zero at low sliding velocities. This reduction of the coefficient of friction can amount to several orders of magnitude. This behavior has been investigated theoretically for the tips of atomic force microscopes (AFM) or friction force microscopes (FFM) and is known as thermolubricity.⁶ In order to obtain the same behavior for the contact between two macroscopic bodies, we propose to shape one of the two surfaces in the form of a vast array of nanopillars with the same mechanical properties as the AFM or FFM tips in terms of typical vibration frequency and amplitude. For

this purpose, it is essential that over distances even as large as centimeters the nanopillars all be produced with precisely the same length and with minimal variation in diameter, so that the number of nanopillars over which the contact forces are distributed is maximized and each nanopillar in the contact has the same mechanical characteristics.

A wide range of literature is available for describing the different methods for producing nanopillar arrays. As an example, the traditional method of so-called “natural lithography”^{7,8} serves as a flexible and affordable technological platform, both technically and economically speaking, that provides good control over the pitch and sharpness of the structures.⁹ On the other hand, it is not possible to avoid irregularities in the pattern of pillars, which do not match the quality that is required for our tribological application. Photography- and holography-based lithography could be effective approaches, but the need for individual masks for each pattern and the low achievable resolution limit the effectiveness of this method.^{10,11} Further, catalytic etching is a fast and versatile method for obtaining vertical submicron structures. However, the resolution and homogeneous separation of the structures still pose challenges.¹² Nanoimprinting¹³ is not a suitable tool due to the difficulty in varying the aspect ratio of the resulting structures. These factors explain our preference for electron beam lithography.^{14–16} Using this method, it is possible to produce large areas of circular patterns with a precision of 2 to 5 nm within a few seconds. Electron beam lithography enables us to manufacture the necessary patterns of nanopillars with sizes up to several square centimeters following the same established recipe while maintaining high quality and reproducibility. With most of the other methods discussed above, it is much more difficult to produce versatile nanopillar arrays on the macroscopic scale.

2 Nanopillar Fabrication

Figure 1 schematically shows the main steps of the nanopillar fabrication process. As substrates, we used 10 × 10 mm pieces of Si(100) wafer (p-type). Prior to processing, samples

*Address all correspondence to: Pavlo V. Antonov, p.antonov@arcnl.nl

†Present address: Advanced Research Center for Nanolithography, Science Park 110, Amsterdam, 1098 XG, The Netherlands.

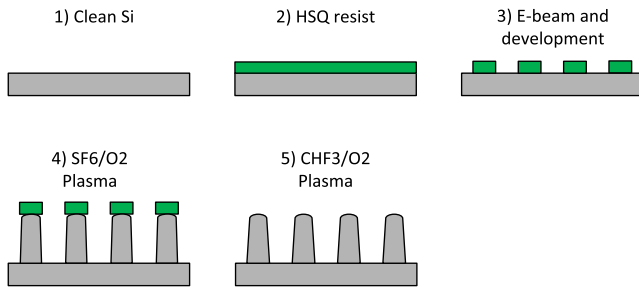


Fig. 1 Schematic of the step-by-step fabrication process of the nanopillar arrays.

were cleaned in two steps. First, they were placed for 5 min in acetone in an ultrasonic bath and were then rinsed with deionized (DI) water. Second, the samples were transferred to a fuming nitric acid (99.9%) HNO_3 bath and kept there for 7 min. They were then rinsed with DI water and dried with N_2 . In order to remove residual moisture, the Si samples were baked for 2 min at 250°C . To achieve a high resolution and high selectivity electron beam pattern generator (EBPG) mask and a subsequent low etch rate,⁷ a negative tone hydrogen silsesquioxane (HSQ) resist was used (XR-1541 Dow Corning, 6% in H_2O). The HSQ resist was first heated to room temperature, after which it was applied directly to the Si substrate, as it did not require any primer due to its strong atomic binding to the substrate. Spin coating was conducted for 55 s at rotation speeds in the range of 4000 to 5500 rpm, depending on the required aspect ratio of the pillars. The final resist layer thickness ranged between 80 nm at low rotation speeds and 60 nm at high speeds.

To obtain a high contrast of lithography, the samples were then baked at 80°C for 4 min. The nanopatterns were written in the HSQ layer by means of a Vistec 5000+ EBPG. The thinnest nanopillars that we have manufactured had a diameter of 50 nm. All patterns were specified by use of the AutoCAD 2013 program, then converted to the corresponding EBPG format. Typically, each of the nanopillar arrays was generated over an area of $50 \times 50 \mu\text{m}$. Optimum resolution was achieved for an electron dose of approximately $1950 \mu\text{C}/\text{cm}^2$ at an acceleration voltage of 100 kV. After exposure, the patterns were developed in a 25% tetramethylammonium hydroxide solution in H_2O for 30 s at a temperature of 80°C . Immediately afterward, the samples were carefully rinsed with DI water for 30 s and flushed with N_2 . We used cryogenic deep reactive ion etching (DRIE) to etch the pillars. This technique is the most powerful and precise method of making high-aspect-ratio objects in Si.^{11,17–19} The etching was carried out in a Adixen AMS-100 Plasma Etcher. The discharge was generated by an RF inductively coupled plasma source directly connected to the working chamber, as shown in Fig. 2. The second RF source was connected directly to the specimen table to provide sufficient directional ion bombardment onto the surface of the sample.

The sample was clamped to a cryogenic holder that was cooled by a flow of liquid N_2 . Helium was back-streamed below the holder in order to provide enough thermal contact between the sample and the holder so as to maintain a precise working temperature of -120°C ($\pm 0.5^\circ\text{C}$). SF_6 was chosen as the working gas, as this provides active fluorine atoms on the sample to react and form an etching product with Si,

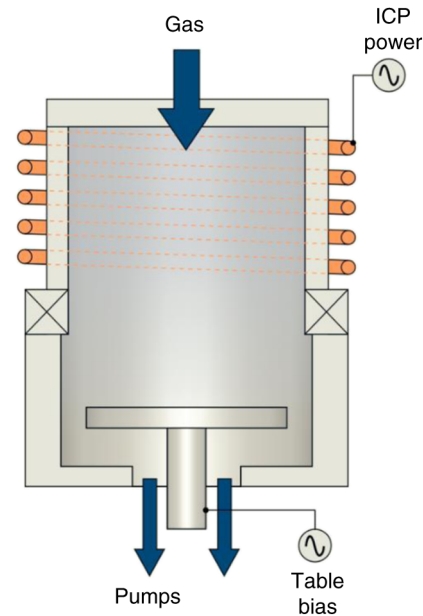


Fig. 2 Schematic of RF inductively coupled plasma system²⁰ used for the deep reactive ion etching of the nanopillar patterns.

which is a volatile SiF_4 . Oxygen was added to the mixture of SF_6 in order to passivate the sidewalls of the vertical structures during etching and thus avoid undercut. The gas flow ratio for this process was established experimentally as $\text{SF}_6:\text{O}_2 = 6.6:1$; specifically, the flow rate of SF_6 was 200 sccm and that of O_2 was 30 sccm, at a total chamber pressure of 6 mbar. An important point to note is that the amount of oxygen could vary as it depended strongly on the size of the structure and the exposed area of the silicon surface. The RF power was set to 1100 W and the bias voltage to -40 V . With these moderate conditions, we achieved a typical etch rate of Si of approximately 2400 nm/min with a selectivity of 80:1 with respect to the HSQ resist. This process produced nanopillar arrays with varying aspect ratios (Fig. 3).

3 Removal of Resist Residues

Because the prime objective of producing these structures was to study their tribological (i.e., frictional) properties, it was also important to have control over the shape of the apex of the pillars. This issue was addressed in combination with the removal of the resist residues that remained on top of the pillars after the DRIE procedure. We considered three options for the removal of the HSQ residues. The first option was to dissolve these residues, which are chemically similar to SiO_2 , in a hydrofluoric acid (HF) solution. We found that a 7% buffered HF solution readily dissolved the HSQ residues, as was expected, but that this treatment had a deleterious effect on the shapes of the pillars, especially for aspect ratios more extreme than 1:12. After HF etching, these had become very rough or were even destroyed completely. Because there was some under-etching effect below the resist, the very top of the pillars had the smallest diameter (see Fig. 3). The second option was therefore to use wet etching of the pillars in order to shrink their diameter uniformly until the residues would detach. It was reported in Ref. 21 that it is possible to slowly and uniformly shrink the diameter of pillars by etching them in dilute aqua

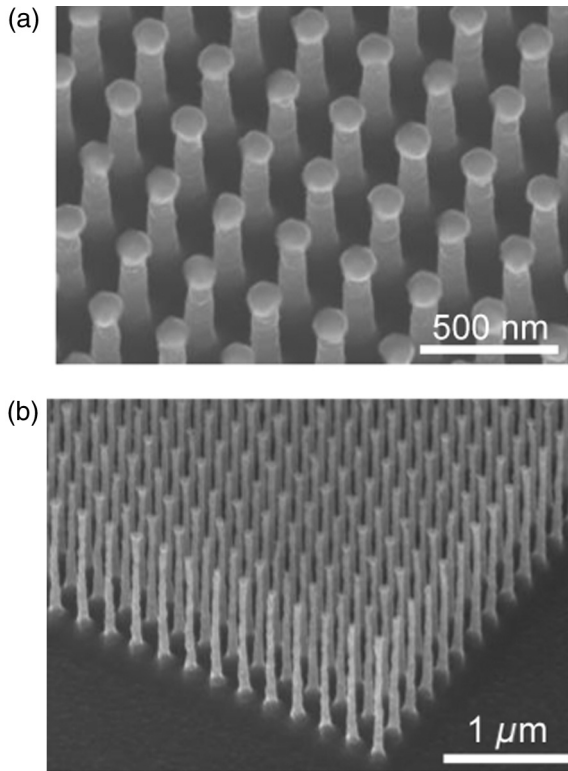


Fig. 3 Scanning electron microscopy images of arrays of Si nanopillars with different aspect ratios. (a) Aspect ratio 1:4, pillar length 400 nm, pillar diameter 95 nm, pitch between centers of pillars 250 nm. (b) Aspect ratio 1:24, pillar length 1.35 μm, pillar diameter 55 nm, pitch 200 nm. Note the resist residue decorating the top of each nanopillar.

regia. In line with the recipe of Ref. 21, we immersed our samples in a solution of $\text{HNO}_3:\text{HCl}:\text{H}_2\text{O} = 1:3:6$ (volume fractions) for approximately 12 h. However, the result showed a negligible etch rate and did not provide any significant changes. We speculate that the DRIE etching at -120°C with O_2 for passivation had provided extra-smooth side interfaces with low densities of chemically active sites, which could have resulted in the negligible effect of dilute aqua regia on the nanopillars.

The third and only successful option was to again resort to the method of plasma etching. Utilizing an inductively coupled CHF_3 plasma in combination with O_2 for passivation provided the required combination of high anisotropy and selectivity between silicon dioxide and silicon. The etching process was conducted in a Leybold Heraeus plasma etcher at room temperature. The following etching parameters were found to achieve the optimal result: a flow of 50 sscm CHF_3 and 2.5 sscm O_2 , 50 W RF power, and -680 V bias voltage at a typical total pressure of 6 to 7 mbar. Under these conditions, the etch rate of silicon dioxide was approximately 36 nm/min, whereas that of silicon was some three times lower. This method allowed us to avoid a bigger undercut and to sharpen the pillars from the top. In Fig. 4, we demonstrate this effect for the example of pillars with an aspect ratio of 1:10. A minor smoothing effect was observed on the pillars during the etching process. We note that this treatment had a deleterious effect on the shapes of pillars with extreme aspect ratios, such as 1:24 (not shown

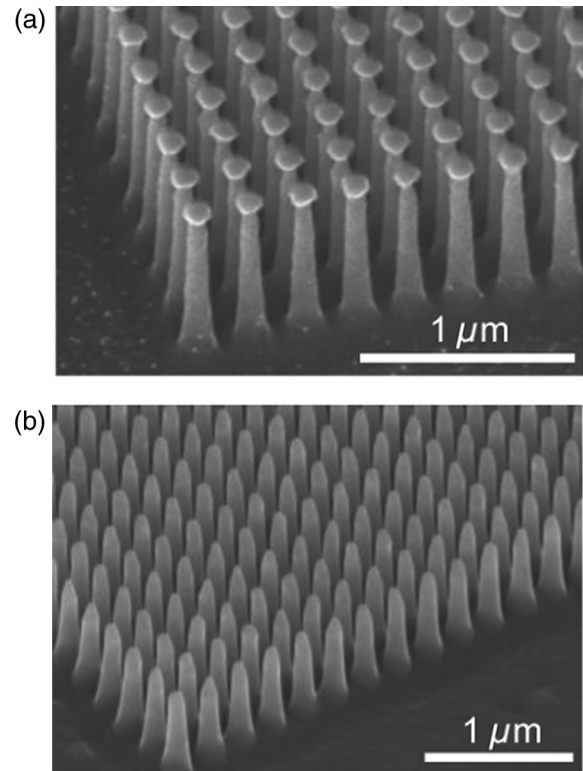


Fig. 4 Scanning electron microscopy images illustrating the effect of CHF_3/O_2 etching. (a) The pillars before etching, with aspect ratio 1:10, pillar length 800 nm, pillar diameter 80 nm, pitch 200 nm. Each pillar is still decorated by a residue of the resist. (b) The result after etching. Note that the resist residues have been removed and that the pillars are slightly rounded at their apex.

here). That is why we decided not to (completely) remove the HSQ residues for those pillars. Depending on the etching time, the average radius of curvature of the apexes of the pillars with aspect ratios less extreme than 1:10 varied from approximately 30 to 12 nm for each specific pattern. This effect is illustrated in Fig. 5 for the case of nanopillars with an aspect ratio of 1:10.

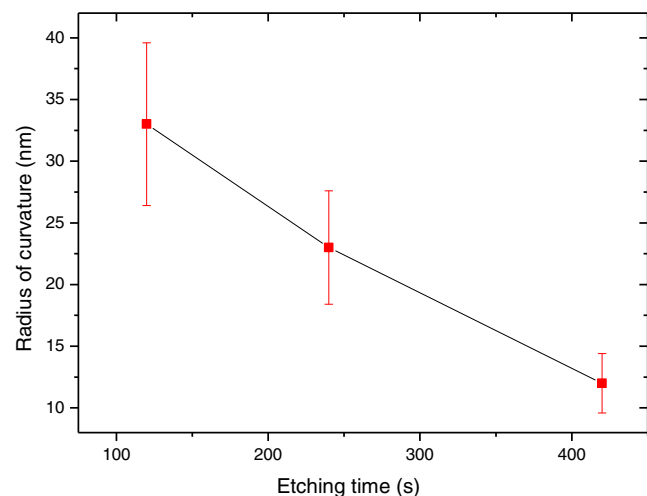


Fig. 5 Average radius of curvature of the apexes of nanopillars with an aspect ratio of 1:10, plotted as a function of the CHF_3/O_2 etching time.

4 Summary

In conclusion, we have shown that an application of DRIE at cryogenic temperatures produces large, absolutely reproducible, and well-ordered arrays of nanopillars with different aspect ratios up to 1:24 over distances of at least 50 μm . We have also applied RIE plasma etching to vary the shape of the pillar apexes by means of etching of the HSQ resist residues. In combination with e-beam lithography, the method shows excellent versatility, anisotropy, and selectivity. The nanostructures produced will be used to study their tribological properties in order to manipulate adhesion and to reduce dry, unlubricated friction.

Acknowledgments

This work was conducted within the context of the “Fundamental Aspects of Friction” project sponsored by the Netherlands Foundation for Fundamental Material Research (FOM) and the ERC-AG project Science F(r)iction. The nanofabrication steps were all conducted at the cleanroom facilities of the Kavli NanoLab at the Delft University of Technology (TUD). The authors would like to express their gratitude to the technical staff of the Kavli NanoLab for their support.

References

1. H. Ko et al., “Multifunctional, flexible electronic systems based on engineered nanostructured materials,” *Nanotechnology* **23**, 344001 (2012).
2. A. M. de Souza Antunes et al., “Trends in nanotechnology patents applied to the health sector,” *Recent Pat. Nanotechnol.* **6**, 29–43 (2012).
3. B. Kiraly, S. K. Yang, and T. J. Huang, “Multifunctional porous silicon nanopillar arrays,” *Nanotechnology* **24**, 245704 (2013).
4. C. K. Chan et al., “High-performance lithium battery anodes using silicon nanowires,” *Nat. Nanotechnol.* **3**(31), 31–35 (2008).
5. D. Liang et al., “High-efficiency nanostructured window GaAs solar cells,” *Nano Lett.* **13**(10), 4850–4856 (2013).
6. S. Yu and J. W. M. Frenken, “The physics of atomic-scale friction: basic considerations and open questions,” *Phys. Status Solidi. B* **251**, 711 (2014).
7. H. W. Deckman and J. H. Dunsmuir, “Nanosphere lithography: a materials general fabrication process for periodic particle array surfaces,” *Appl. Phys. Lett.* **41**, 377 (1982).
8. L. Chitu et al., “Modified Langmuir-Blodgett deposition of nanoparticles—measurement of 2D to 3D ordered arrays,” *Meas. Sci. Rev.* **10**(5) (2010).
9. C.-M. Hsu et al., “Wafer-scale silicon nanopillars and nanocones by Langmuir-Blodgett assembly and etching,” *App. Phys. Lett.* **93**, 133109 (2008).
10. T. Ito and S. Okazaki, “Pushing the limits of lithography,” *Nature* **406**(6799), 1027–1031 (2000).
11. Y.-J. Hung et al., “Fabrication of highly-ordered silicon nanowire arrays with controllable sidewall profiles for achieving low surface reflection,” *Mater. Res. Soc. Symp. Proc.* 869–877 (2010).
12. Z. Huang, H. Fang, and J. Zhu, “Fabrication of silicon nanowire arrays with controlled diameter, length, and density,” *Adv. Mater.* **19**, 744–748 (2007).
13. C. M. S. Torres et al., “Nanoimprint lithography: an alternative nanofabrication approach,” *Mater. Sci. Eng. C* **23**, 23–31 (2003).
14. C. Vieu et al., “Electron beam lithography: resolution limits and applications,” *App. Surf. Sci.* **164**, 111–117 (2000).
15. B. Kaleli et al., “Electron beam lithography of HSQ and PMMA resists and importance of their properties to link the nano world to the micro world,” presented at *Proc. STW ICT Conf.*, 18–19 November 2010, Veldhoven, The Netherlands.
16. A. E. Grigorescu, M. C. van der Krogt, and C. W. Hagen, “Limiting factors for electron beam lithography when using ultra-thin hydrogen silsesquioxane layers,” *J. Micro/Nanolith. MEMS MOEMS* **6**(4), 043006 (2007).
17. S. Tachi, K. Tsujimoto, and S. Okudaira, “Low-temperature reactive ion etching and microwave plasma etching of silicon,” *Appl. Phys. Lett.* **52**(8), 616–618 (1988).
18. Z. Liu et al., “Super-selective cryogenic etching for sub-10 nm features,” *Nanotechnology* **24**, 015305 (2013).
19. M. Boufnichel et al., “Profile control of high aspect ratio trenches of silicon. Effect of process parameters on local bowing,” *J. Vac. Sci. Technol. B* **20**, 1508–1513 (2002).
20. Oxford Instruments, “Image of inductively-coupled plasma reactor,” <http://www.oxford-instruments.com/products/etching-deposition-and-growth/plasma-etch-deposition/icp-etch>.
21. Y.-F. Chang et al., “Fabrication of high-aspect-ratio silicon nanopillar arrays with the conventional reactive ion etching technique,” *Appl. Phys. A* **86**, 193–196 (2007).

Pavlo V. Antonov is a PhD student at the Advanced Research Center of Nanolithography. He received his BSc and MSc degrees from Kharkov National University, Ukraine, in 2010 and 2012, respectively. His current research interests include tribology of graphene and thin films, superlubricity, and nanolithography.

Biographies for the other authors are not available.